ChemComm

Complete Denitrification of Nitrate and Nitrite to N_2 gas by Samarium(II) Iodide

Journal:	*ChemComm*
Manuscript ID	CC-COM-06-2020-004115.R2
Article Type:	Communication

COMMUNICATION

Complete Denitrification of Nitrate and Nitrite to N_2 gas by Samarium(II) Iodide

Received 00th January 20xx,
Accepted 00th January 20xx

DOI: 10.1039/x0xx00000x

Walker R. Marks,[a] Douglas F. Baumgardner,[a] Eric W. Reinheimer,[b] and John D. Gilbertson[a]

The reduction of nitrogen oxides ($N_xO_y^{n-}$) to dinitrogen gas by samarium(II) iodide is reported. The polyoxoanions nitrate (NO_3^-) and nitrite (NO_2^-), as well as nitrous oxide (N_2O) and nitric oxide (NO) were all shown to react with stoichiometric amounts of SmI_2 in THF for the complete denitrification to N_2.

Nitrate (NO_3^-) and nitrite (NO_2^-) play a vital role in the global nitrogen cycle.[1,2] Through human intrusions such as the persistent use of fertilizers, the equilibrium/disequilibrium that has historically governed this cycle is collapsing, causing environmental crises on the global scale.[3,4] For example, nitrous oxide (N_2O), which is an important intermediate in denitrification cycles, is a leading cause of both global warming and ozone layer depletion.[5,6] In addition, eutrophication in aquatic ecosystems is often related to pollution from nitrites and nitrates.[7] This eutrophication leads to the formation of so-called "hypoxic" or "dead zones" in which plant and animal life is unsustainable due to the depleted oxygen levels. Clearly, systems capable of complete denitrification, defined here as the reduction of NO_3^-/NO_2^- to benign N_2, are needed.

To date, there are no homogeneous[8-10] or heterogeneous NO_3^- denitrification schemes based on lanthanide catalysts (or electrocatalysts[11,12]) and only one system that we are aware of (based on NiPNP)[13] that can achieve complete denitrification on a single metal-ligand scaffold. Similar to the initial report of the molybdenum-mediated O-atom transfer from nitrate,[14] O-atom extraction from nitrogen oxyanions via the Mashima[15] or borylating[16] reagents, as well as through the use of oxygen-deficient polyoxo-clusters,[17] have recently been shown to be viable strategies for selective (albeit incomplete) denitrification. Additionally, the inner sphere reduction[18,19] of NO_3^- via Ce(III) complexes provides a glimpse into the utility of lanthanides for denitrification. In this spirit we reasoned that other oxophilic[20] lanthanides may also be useful in the O-atom transfer from NO_x^{n-}.

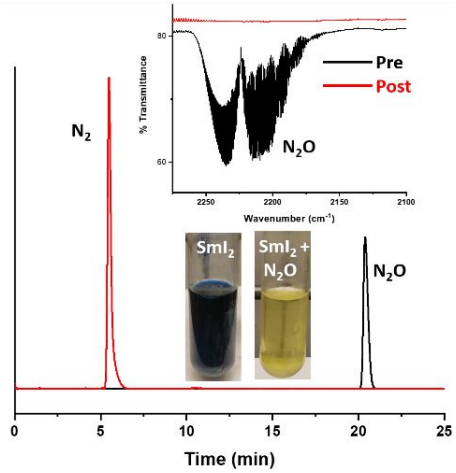

Fig. 1 GC trace and gas phase FTIR (inset) of the headspace of the reaction (tubes) of SmI_2 with N_2O in THF.

Samarium in the form of Sm(II) iodide is well known in the realm of electron transfer reactions as one of the most versatile electron transfer reagents available.[21,22] Furthermore, Sm(II) has been reported in the reduction of aryl and alkyl nitro compounds to form N-N bonds in the form of hydrazines, azoarenes, or azoxyarenes.[23,24] In addition, the organometallic complex $(Cp^*)_2Sm(THF)_2$ is one of the most powerful reductants known,[25] capable of dinitrogen activation.[26] As an O-atom acceptor, $(Cp^*)_2Sm(THF)_2$ has been reported[27] to react with NO and N_2O to form the bridging μ-oxo $[(Cp^*)_2Sm]_2(\mu\text{-}O)$. Lastly, $Sm(II)(OTf)_2(dme)_2$ has been shown[28] to form tetrametallic assemblies of Sm(III) upon reaction with N_2O. In each of those examples, the fate of the nitrogen atoms is still unresolved. Here we report the complete denitrification of the nitrogen oxides NO_3^-, NO_2^-, N_2O, and NO to N_2 gas with SmI_2 in THF.

Stirring two equivalents of ~0.1 M SmI_2 in THF with one equivalent of N_2O in the dark over a 48-hour period results in a

[a] *Department of Chemistry, Western Washington University, Bellingham, Washington 98225, United States Email: john.gilbertson@wwu.edu*
[b] *Rigaku Oxford Diffraction, Woodlands TX 77381, United States*
Electronic Supplementary Information (ESI) available: [Complete experimental details, spectroscopic (GC, FTIR, HPIC, MS, UV-vis) and X-ray crystallographic data.]. *CCDC 2009513- 2009515*. See DOI: 10.1039/x0xx00000x

color change from a deep blue to translucent yellow (Figure 1). The reactions were run in air-free side-arm flasks that were initially charged with SmI_2/THF and degassed via three consecutive rounds of freeze-pump-thaw before N_2O was layered onto the frozen solutions at 77 K. The vessel was then allowed to warm and stir for two days at ambient temperature after which the solution had turned from deep blue to pale yellow. Investigation of the headspace via FTIR spectroscopy reveals complete consumption of the N_2O gas. As shown in Figure 1, a GC trace of the headspace shows that the only gaseous product is N_2, detected in near quantitative yield (Table 1). Neither the pre- nor post-reaction GC trace(s) contain peaks for O_2, indicating a leak free system. Removal of the THF solvent results in a yellow solid that when redissolved in CH_3CN and allowed to evaporate, yields yellow crystals of the autoionized $SmI_3.(THF)_x$ compound (**1**) $[SmI_2(THF)_5][SmI_4(THF)_2]$.[29] As in the previous report of the formation of **1** from the oxidation of SmI_2 with dioxygen in a THF solution, both Sm centers are in the +3 oxidation state, indicating that each Sm^{2+} is a one electron reductant in the N_2O reduction scheme.

Table 1. Selected reaction yields of Sm^{2+} and $N_xO_y^{n-}$.

Sm^{2+}: $N_xO_y^{n-}$	$N_xO_y^{n-}$	Gaseous products	% yield N_2[a]	% $N_xO_y^{n-}$ consumed
2:1	N_2O	N_2	97 +/- 4	100
1:1	N_2O	N_2	65 +/- 3	69
4:1	NO_2-	N_2	66 +/- 7	100
1:1	NO_2-	N_2, NO, N_2O	[b]151 +/- 8	[d]97
			[c]51 +/- 2	[d]97
6:1	NO_3-	N_2	80 +/- 8	[d]100
1:1	NO_3-	N_2, N_2O	[b]66 +/- 6	[d]14
			[c]14 +/- 2	[d]14

[a] Calculated from GC. [b]Based on SmI_2. [c]Based on $N_xO_y^{n-}$. [d] Calculated from IC, reported to +/- 2%.

A mass spectrum (Figure S3) provides evidence of the fate of the oxygen atom in the N_2O reduction reaction. In addition to the doubly ionized $[SmI(CH_3CN)_3]^{2+}$ and $[SmI(CH_3CN)_4]^{2+}$ at m/z = 199 and 220, respectively, a m/z of 309 was detected, corresponding to $[Sm(O)(CH_3CN)_3(H_2O)]^+$. There were two additional major species that displayed the diagnostic Sm^{3+} isotopic pattern at 569 and 588 m/z, respectively. These m/z are attributed to $[SmI_2(CH_3CN)_4]^+$ and $[SmI_2(CH_3CN)_4(H_2O)]^+$. The relative intensities of the total singly ionized species $[Sm^{3+}]$ to $[Sm(O)^+]$ detected also indicate that those species are present in ~1:1 ratio. In addition, reacting SmI_2 directly with O_2 in THF[30] yields a near identical mass spectrum (Figure S17), resulting in the $[Sm(O)(CH_3CN)_3(H_2O)]^+$ species, confirming the precedent for the formation of the oxyhalide SmOI.[31] These data suggest the stoichiometry in equation 1 for the reduction of N_2O by SmI_2.

$$2\ SmI_2 + N_2O \rightarrow SmI_3 + SmOI + N_2 \qquad (\mathbf{1})$$

Redissolution of the yellow product mixture in wet acetone and allowing slow evaporation of the solvent provided X-ray quality crystals of the $[Sm_6(\mu_3\text{-}OH)_8(\mu_6\text{-}O)(H_2O)_{24}][I_8]$ cluster (**2**) shown in Figure 2. The cluster crystallized in the centrosymmetric, orthorhombic space group *Pnnm* and consists of one-quarter of the distorted octahedral cluster of trivalent samarium atoms. Each of the samarium atoms is bound to triple-bridged oxygen atoms and a central oxygen atom. The coordination environment around each Sm^{3+} is completed by four coordinated water molecules. Inspection of the Sm-O distances within the cluster between the three samarium atoms in the asymmetric unit and O(11) (the central oxygen atom in the octahedral cluster) were measured at 2.58401(8), 2.56579(5), and 2.56247(9) Å respectively while those between the samarium atoms and the triply-bridged oxygen atoms ranged from 2.37910(5) - 2.39786(4) Å. These bond distances are similar to other Sm-oxo clusters reported.[32,33] The triply bridged oxygen atoms are assigned as μ_3-OH groups, based on successive least-squares refinement of the X-ray crystallographic data for **2**, which revealed peaks in the difference map suggestive of hydrogen atoms bound to the bridging oxides. As a direct result, the formula for the cluster with water molecules bound is $[Sm_6(\mu_3\text{-}OH)_8(\mu_6\text{-}O)(H_2O)_{24}]^{8+}$ with the charge balanced by eight iodide anions. A similar $[Sm_6(\mu_3\text{-}OH)_8(\mu_6\text{-}O)(CH_3CN)_2(H_2O)_{6.8}(C_3H_6O)_{11.2}]^{8+}$ cluster (**3**) with acetonitrile and acetone ligands in the place of the aqua ligands is obtained upon recrystallization from a mixture of THF/acetonitrile/acetone and can be found in the Supporting Information.

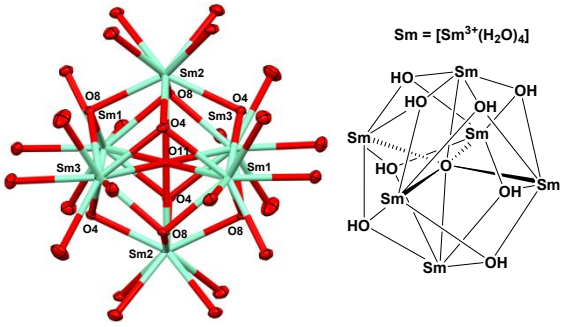

Fig. 2 Solid state structure (left) and Chemdraw (right) of $[Sm_6(\mu_3\text{-}OH)_8(\mu_6\text{-}O)(H_2O)_{24}]^{8+}$. The H-atoms of the μ_3-hydroxos and the H-atoms of terminal aqua ligands have been omitted from the ORTEP for clarity. Thermal ellipsoids are shown at 50%.

After establishing SmI_2 as a viable reductant for N_2O we further explored the reactivity in the denitrification scheme of oxyanions such as NO_3^- and NO_2^-. As can be seen from equations 1-3 and Table 1, Sm^{2+} is a capable of the multielectron conversion(s) from $N_xO_y^{n-}$ to N_2. Reaction of excess SmI_2 with the nitrate salts $TBANO_3$ (where TBA = tetrabutylammonium) or KNO_3 in THF in 6:1 ratios Sm^{2+}:NO_3^- results in complete consumption of the nitrate anions as indicated by ion chromatography (Figure S7). In order to eliminate any contamination from atmospheric nitrogen, all reactions were set-up and run in an argon-filled glovebox using air-free side-arm flasks. The SmI_2/THF solutions were degassed via three consecutive freeze-pump-thaw cycles before being exposed to the Ar box atmosphere. Headspace analysis via both FTIR and GC also reveal N_2 as the only

gaseous product in the reaction, resulting in the stoichiometry presented in equation 2.

$$5\ Sm^{2+} + NO_3^- \rightarrow 2\ Sm^{3+} + 3\ SmO^+ + \tfrac{1}{2}\ N_2 \quad (\mathbf{2})$$

GC traces of the pre- and post-reaction show no O_2 peaks indicating the system is free from leaks.[34] As stated above, Table 1 indicates that complete consumption of NO_3^- by IC, and no other N-containing ions are detected in the products. However, the yield observed in N_2 is only ~80%. We hypothesize that the remaining 20% is due to gas loss during the instantaneous reaction during the syringe transfer of the solutions of SmI_2/THF onto the NO_3^- salt.[30] Mass spectra (Figure S8) also indicate the diagnostic peaks due to $[Sm(O)]^+$ and $[Sm^{3+}]$ as observed in the N_2O reductions. Isotopic labeling studies using $^{15}NO_3^-$ in the starting salt results in a clean ^{15}N NMR spectrum showing $^{15}N_2$ as the only ^{15}N-containing product (Fig. S25). If the NO_3^- reactions are run with Sm^{2+} as the limiting reagent in a 1:1 ratio, the gaseous product N_2O is also detected in the headspace, suggesting that N_2O is an intermediate in the nitrate reduction reaction. Additionally, isotopic labeling studies using $^{15}NO_3^-$ in the starting salt results in $^{15}N_2O$ in the FTIR spectrum and $^{15}N_2$ in the ^{15}N NMR spectrum (Fig. S5).

When the salts $TBANO_2$ and/or $NaNO_2$ are used in place of the nitrate salts, and the Sm^{2+}:NO_2^- ratios are adjusted to 4:1, identical results are obtained, and we observe conversion of NO_2^- to N_2 according to equation 3. The reactions are run in identical fashion to the NO_3^- reactions described above, in order to eliminate any nitrogen contamination. As in the excess NO_3^- reactions, quantitative detection of N_2 is not observed, due to presumed gas loss during initial mixing. Isotopic labeling studies using $^{15}NO_2^-$ in the starting salt results in a clean ^{15}N NMR spectrum showing $^{15}N_2$ as the only ^{15}N-containing product (Fig. S25).

$$3\ Sm^{2+} + NO_2^- \rightarrow Sm^{3+} + 2\ SmO^+ + \tfrac{1}{2}\ N_2 \quad (\mathbf{3})$$

Interestingly, when Sm^{2+} is the limiting reagent and the NO_2^- reactions are run in a 1:1 ratio, in addition to N_2, the gaseous products NO and N_2O are also detected in the headspace. Isotopic labeling studies using $^{15}NO_2^-$ in the starting salt results in a mixture of $^{15}N_2O$ and ^{15}NO in the FTIR spectrum (Fig. S10). The yield of N_2 w/ respect to Sm^{2+} is ~150%, clearly indicating that there is another source of electrons available in the reaction. A positive starch/iodine test of the reaction mixture reveals the presence of I_2, indicating that I^- is also a source of electrons in the reduction of NO_2^- to NO, as shown in equation 4. This is a standard method[35] for the production of NO from acidic solutions of NO_2^- and I^- (presumably Sm(III) acts as a Lewis acid in this case). Control experiments[30] also show that NO is a competent substrate for reduction to N_2O and N_2. A thiosulfate titration of the resultant reaction mixture allowed us to quantify the electrons provided by the iodide ions, which accounted for the extra two equivalents. The yield based on electron utilization from Sm(II) in the 1:1 SmI_3:NO_2^- is then 51 +/- 2% N_2.

$$2\ I^- + 2NO_2^- + \text{acid} \rightarrow 2\ NO + I_2 + 2\ O^{2-} \quad (\mathbf{4})$$

These results provide some insight in to how the SmI_2 reduces the polyoxoanions. Typically, in Nature, four separate, distinct metalloenzymes are required for the five-electron denitrification of nitrate to dinitrogen[1,36,37] in a series of one and two electron processes according to Scheme 1 (black arrows).

Scheme 1. Denitrification of NO_3^- to N_2 with four different metalloenzymes (black arrows) and SmI_2 (red arrows).

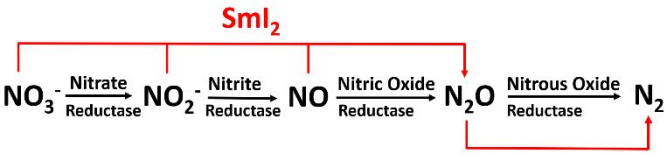

The first step in the cycle is a two electron reduction carried out by nitrate reductase to form NO_2^-. The NO_2^- is then reduced via a series of separate, one and two electron reductions to ultimately form N_2. Sm(II) is a single electron transfer (SET) agent and the reduction of oxides such as NO and N_2O by Sm(II) involves two SET from separate centers followed by oxygen atom transfer (OAT) resulting in a dinuclear compound with a bridging oxide.[27,38] In deoxygenation reactions by SmI_2, the initial reaction product "$I_2SmOSmI_2$" is proposed to decompose into SmI_3 and SmOI,[31] consistent with our MS studies described above.

In the case of denitrification by SmI_2, two SETs to NO_3^-, followed by an OAT would result in NO_2^-, similar to nitrate reductase in Nature. However, NO gas is not detected in the NO_3^- reductions reactions, which would clearly be present due to the I^-/NO_2^- reactivity described in equation 4 (a starch/iodine test also is negative for the presence of I_2). On the other hand, NO_2^- is a competent substrate for reduction by SmI_2 as shown in equation 3, so if NO_2^- is an intermediate, it is clearly short-lived. An alternate possibility is that OAT occurs after one SET event in the denitrification of NO_3^- to yield NO_2. Even though we do not observe NO_2 in the headspace, at this point we cannot rule out this intermediate, as previous reports[18] of the inner sphere reduction of NO_3^- by the lanthanide Ce(III) are proposed to produce NO_2, although no evidence for the detection of NO_2 was presented in that work as well. Both routes would result in an NO^{n-} species (either NO^- or NO) from further SET/OAT which can couple to form hyponitrite[39,40] ($N_2O_2^{2-}$) with subsequent disproportionation to form N_2O.[41] Similar routes to N_2O have been proposed for the reduction of NO to N_2O on low-valent uranium,[42] and other early metal[43] reductions to N_2O. Regardless, we are continuing to explore the mechanism of these reactions, in addition to methods of regenerating Sm(II) from the Sm(III) containing product species. In spite of its usefulness,[44] very little progress has been made to date in terms of incorporating Sm into catalytic cycles, due to the difficulty of regenerating Sm(II).[45-50]

Conclusions

In conclusion, SmI_2 is capable of performing the complete, stoichiometric denitrification of nitrogen oxides to dinitrogen gas. To the best of our knowledge, this is the first report of the complete denitrification of the polyoxoanions NO_3^- and NO_2^- utilizing a lanthanide complex. This report further illustrates the versatility of Sm(II) as both a SET and an OAT agent, as the general utility is demonstrated by the cascade of tandem

polyoxoanion deoxygenations via multiple SET and OAT events, all in a single reaction vessel.

This research was supported by an award from the National Institute of Health (R15GM123380 to JDG), NSF MRI awards (CHE-1429164 and CHE-1532269), and an award from WWU RSP (DFB). JDG is a Henry Dreyfus Teacher Scholar. We thank Sam Danforth (WWU) for assistance with crystallographic data collection, WWU Scitech for assistance with HPIC, and Prof. John Antos (WWU) for assistance with MS data collection and analysis.

Conflicts of interest

There are no conflicts to declare.

References

1 L. B. Maia and J. J. G. Moura, *Chem. Rev*., 2014, **114**, 5273.
2 A. J. Timmons and M. D. Symes, *Chem. Soc. Rev*., 2015, **44**, 6708.
3 S. Fields, *Environ. Health Perspect*., 2004, **112**, A556.
4 M. H. Ward, T. M. deKok, P. Levallois, J. Brender, G. Gulis, ; B. T. Nolan and J. VanDerslice, *Environ. Health Perspect*., 2005, **113**, 1607.
5 A. R. Ravishankara, J. S. Daniel and R. W. Portmann, *Science,* 2009, **326**, 123.
6 A. J. Thomson, G. Giannopoulos, J. Pretty, E. M. Baggs and D. J. Richardson, *Philos. Trans. R. Soc. London Ser. B,* 2012, **367**, 1157.
7 D. W. Schindler, *Science,* 1974, **184**, 897.
8 C. L. Ford, Y. J. Park, E. M. Matson, Z. Gordon and A. R. Fout, *Science,* 2016, **354**, 741.
9 Y. Guo, J. R. Stroka, B. Kandemir, C. E. Dickerson and K. L. Bren, *J. Am. Chem. Soc*., 2018, **140**, 16888.
10 S. Xu, D.C. Ashley, K.-Y. Kwon, G.R. Ware, C.-H. Chen, Y. Losovyj, X. Gao, E. Jakubikova and J.M. Smith, *Chem. Sci*., 2018, **9**, 4950.
11 M. Duca and M. T. M. Koper, *Energy Environ. Sci.,* 2012, **5**, 9726.
12 J.-X. Liu, D. Richards, N. Singh and B. R. Goldsmith, *ACS Catal.,* 2019, **9**, 7052.
13 J. Gwak, S. Ahn, M.-H. Baik and Y. Lee, *Chem. Sci.,* 2019, **10**, 4767.
14 J. A. Craig and R. H. Holm, *J. Am. Chem. Soc*., 1989, **111**, 2111.
15 J. Seo, A. C. Cabelof, K. G. Caulton and C. Chen, *Chem. Sci*., 2019, **10**, 475.
16 D. M. Beagan, V. Carta and K. G. Caulton, *Dalton Trans.,* 2020, **49**, 1681.
17 B. E. Petel and E. M. Matson, *Chem. Commun.,* 2020, **56**, 555.
18 P. L. Damon , G. Wu, N. Kaltsoyannis and T. W. Hayton, *J. Am. Chem. Soc*., 2016, **138**, 12743.
19 M. K. Assefa, G. Wu and T. W. Hayton, *Chem. Sci*., 2017, **8**, 7873.
20 K. P. Kepp, *Inorg. Chem.,* 2016, **55**, 9461.
21 M. Szostak and D. J. Procter, *Angew. Chem. Int. Ed.* 2012, **51**, 9238.
22 D. J. Procter, R. A. Flowers II and T. Skrydstrup, *Organic Synthesis and using Samarium Diiodide: A Practical Guide,* RSC Publishing, 2009.
23 J. Souppe, L. Danon, J. L. Namy and H. B. Kagan, *J. Organomet. Chem*., 1983, **250**, 227.
24 E. D. Brady, D. L. Clark, D. W. Keogh, B. L. Scott and J. G. Watkin, *J. Am. Chem. Soc*., 2002, **124**, 7007.
25 W. J. Evans, S. L. Gonzales and J. W. Ziller, *J. Am. Chem. Soc.,* 1994, **116**, 2600.
26 W. J. Evans and D. S. Lee, *Can. J. Chem*, 2005, **83**, 375.
27 W. J. Evans, J. W. Grate, I. Bloom, W. E. Hunter, J. L. Atwood, *J. Am. Chem. Soc.,* 1985, **107**, 405.
28 M. Xémard, M. Cordier, E. Louyriac, L. Maron, C. Clavaguéra and G. Nocton, *Dalton Trans.,* 2018, **47**, 9226.
29 Z. Xie, K.-Y. Chiu, B. Wu and T. C. W. Mak, *Inorg. Chem*., 1996, **35**, 5957.
30 See Supporting Information for experimental details.
31 J. Prandi, J. L. Namy, G. Menoret and H. B. Kagan, *J. Organomet. Chem*., 1985, **285**, 449.
32 W. J. Evans, N. T. Allen, M. A. Greci and J. W. Ziller, *Organometallics,* 2001, **20**, 2936.
33 O. T. Summerscales, D. R. Johnston, F. G. N. Cloke and P.B. Hitchcock, *Organometallics*, 2008**, 27**, 5612-5618.
34 The GC experiments utilized argon as the carrier gas to allow the detection and discrimination between any potential leak (O_2) and the reaction box atmosphere (Ar). See Supporting Information for details.
35 A. Mayburd and R. J. Kassner, *Biochemistry,* 2002, **41**, 11582.
36 C. Sparacino-Watkins , J. F. Stolz and P. Basu , *Chem. Soc. Rev.*, 2014, **43** , 676.
37 I. M. Wasser, S. de Vries, P. Moënne-Loccoz, I. Schröder and K. D. Karlin, *Chem. Rev*., 2002, **102**, 1201.
38 M. Xémard, M. Cordier, E. Louyriac, L. Maron, C. Clavaguéra and G. Nocton, *Dalton Trans.,* 2018, **47**, 9226.
39 Y. Arikawa and M. Onishi, *Coord. Chem. Rev.,* 2012, **256**, 468.
40 A. M. Wright and T. W. Hayton, *Inorg. Chem.,* 2015, **54**, 9330.
41 M. P. Schopfer, J. Wang and K. D. Karlin, *Inorg. Chem.,* 2010, **49**, 6267.
42 C. J. Hoerger, H. S. La Pierre, L. Maron, A. Scheurer, F. W. Heinemann and K. Meyer, *Chem. Commun.,* 2016, **52**, 10854.
43 K. McNeill and R. G. Bergman, *J. Am. Chem. Soc*., 1999, **121**, 8260.
44 M. Szostak, M. Spain and D. J. Procter, *Chem. Soc. Rev.,* 2013, **42**, 9155.
45 S. Maity and R. A. Flowers II, *J. Am. Chem. Soc.,* 2019, **141**, 3207.
46 E. J. Corey and G. Z. Zheng, *Tetrahedron Lett*., 1997, **38**, 2045.
47 F. Orsini and E. M. Lucci, *Tetrahedron Lett*. **2005**, *46*, 1909–1911.
48 Lannou, M. I.; Hélion, F.; Namy, J. L. Some Uses of Mischmetal in Organic Synthesis. *Tetrahedron,* 2003, **59**, 10551.
49 Y. F. Zhang and M. Mellah, *ACS Catal*., 2017, **7**, 8480.
50 L. Sun, K. Sahloul and M. Mellah, *ACS Catal*., 2013, **3**, 2568.

Complete Denitrification of Nitrate and Nitrite to N_2 gas by Samarium(II) Iodide

Walker R. Marks, Douglas F. Baumgardner, Eric W. Reinheimer, and John D. Gilbertson